

# Efficient Method for the Calculation of Dissipative Quantum Transport in Quantum Cascade Lasers

Stefan Birner<sup>1,2</sup>, Peter Greck<sup>2</sup> and Peter Vogl<sup>2</sup>

<sup>1</sup> nextnano GmbH, 85586 Poing, Germany

<sup>2</sup> Walter Schottky Institut, Physik-Department, Technische Universität München, Am Coulombwall 4, 85748 Garching, Germany  
stefan.birner@nextnano.com

## 1. Abstract

We present a novel and very efficient method for calculating quantum transport in quantum cascade lasers (QCLs). It follows the nonequilibrium Green's function (NEGF) framework but sidesteps the calculation of lesser self-energies by replacing them by a quasi-equilibrium expression. This method generalizes the phenomenological Büttiker probe model [1] but takes into account all relevant individual scattering mechanisms. It is orders of magnitude more efficient than a fully self-consistent NEGF calculation for realistic devices, yet accurately reproduces the results of the latter. We apply this method to a new THz QCL design which works up to 250 K – according to our simulations. Our algorithm has been implemented into the nextnano.MSB software (www.nextnano.com) and allows finding an optimal QCL layout very quickly, as variations in alloy concentration, barrier thickness, and further parameters can be calculated in parallel.

## 2. Introduction

A detailed understanding of carrier dynamics is crucial for the design and improvement of modern semiconductor nanodevices such as QCLs. However, neither a classical or semiclassical nor a strictly coherent, ballistic quantum mechanical theory can capture the tight interplay between incoherent relaxation processes and quantum interference effects. In this work, we present a novel method to calculate stationary quantum transport properties that we termed multi-scattering Büttiker probe model (MSB) [2]. The standard Büttiker probe scattering model associates a single momentum and energy sink with each device grid point. In contrast, our new MSB model accounts for individual scattering mechanisms by using multiple probes for each grid point.

## 3. Method

A full implementation of the NEGF method requires the self-consistent solution of the retarded and lesser Green's functions,  $\mathbf{G}^R$  and  $\mathbf{G}^<$ . The first one characterizes the width and energy of the scattering states, whereas the second quantity characterizes the state occupancy and determines the charge and current density. The self-consistent solution cycle involves the solution of four coupled integro-differential equations,

$$\mathbf{G}^R = (E - \mathbf{H}_D - e\varphi - \Sigma^R)^{-1}, \quad (1)$$

$$\Sigma^R = \mathbf{G}^R \mathbf{D}^R + \mathbf{G}^R \mathbf{D}^< + \mathbf{G}^< \mathbf{D}^R, \quad (2)$$

$$\Sigma^< = \mathbf{G}^< \mathbf{D}^<, \quad (3)$$

$$\mathbf{G}^< = \mathbf{G}^R \Sigma^< \mathbf{G}^{R\dagger}, \quad (4)$$

where  $\mathbf{H}_D$  is the electronic device Hamiltonian and  $\varphi$  is the electrostatic potential that needs to be solved by the Poisson equation self-consistently with the Green's functions.  $\Sigma^R$ ,  $\Sigma^<$  are the scattering self-energies, and  $\mathbf{D}^R$ ,  $\mathbf{D}^<$  represent the environmental Green's functions that contain the scattering variables. All quantities are functions of space, momentum and energy. For a multi-quantum well structure such as a QCL grown along the  $z$  axis, the lateral momentum conservation simplifies the arguments to the following functional form,  $\mathbf{G} = \mathbf{G}(z, z', k_{\parallel}, E)$ . The key simplifications in our new MSB approach consist in (i) sidestepping the self-consistent solution of  $\Sigma^<$  and  $\mathbf{G}^<$  and

(ii) performing the  $k_{\parallel}$  integration analytically so that the Green's functions become functions of space and energy only,  $\mathbf{G} = \mathbf{G}(z, z', E)$ . Now the self-consistent cycle only involves two equations, namely eq. (1) and  $\Sigma^R = \mathbf{G}^R \mathbf{D}^R$ . The self-energy  $\Sigma^R$  includes scattering due to acoustic and optical phonons and the coupling to the contacts. The lesser Green's function  $\mathbf{G}^<$  is calculated by using the expression for an equilibrium system,

$$\mathbf{G}^< = F_0(\mathbf{G}^R - \mathbf{G}^{R\dagger}), \quad (5)$$

albeit with Fermi integral  $F_0(z, E)$  that contains a local Fermi level  $\mu(z)$  which is determined in such a way as to guarantee current conservation,  $\text{div } \mathbf{j} = 0$ .

#### 4. Results

We propose and simulate a novel two-well injectorless GaAs/AlGaAs THz QCL design with a photon emission frequency of 2.85 THz ( $\hbar\omega = 11.8$  meV). Remarkably, we calculate gain up to 250 K. This high temperature operation is confirmed by a complementary, independent simulation based on a different NEGF code [3,4]. Our previous simulations of a few other common THz QCL designs do not show such a high temperature operation, in agreement to experiment. The layer sequence for one period is **2.1/7.35/2.1/7.35** nm (**Al<sub>0.1</sub>Ga<sub>0.9</sub>As/GaAs/Al<sub>0.26</sub>Ga<sub>0.74</sub>As/GaAs**). Barriers are shown in bold. Only the underlined GaAs region is doped with  $3 \cdot 10^{16} \text{ cm}^{-3}$ . We do not impose the restriction of uniform barrier heights, i.e. we use different aluminum contents which correspond to conduction band offsets of 107 meV and 237 meV, respectively. We find that the gain is not very sensitive with respect to layer thickness fluctuations. The operation scheme of this proposed QCL can be seen from Fig. 1. The design consists of alternating upper and lower laser states only. Fig. 1(a) shows the local density of states. The upper states are labeled '1a' and '2a'. From this upper laser level a diagonal photon transition into the states '1b' and '2b', respectively, is possible. The majority of carriers are efficiently thermalized from state '1a' into the upper laser state '2a' of the next period because their energy difference is designed to be the energy of a longitudinal optical (LO) phonon (34 meV in GaAs). Our design pushes the higher lying states like '1u' and '2u' about 175 meV above the conduction band edge. Thus, they do not interact and interfere with other states of previous periods. Fig. 1(b) shows that they do not carry any significant current. We find that almost the complete period contributes to the optical gain.

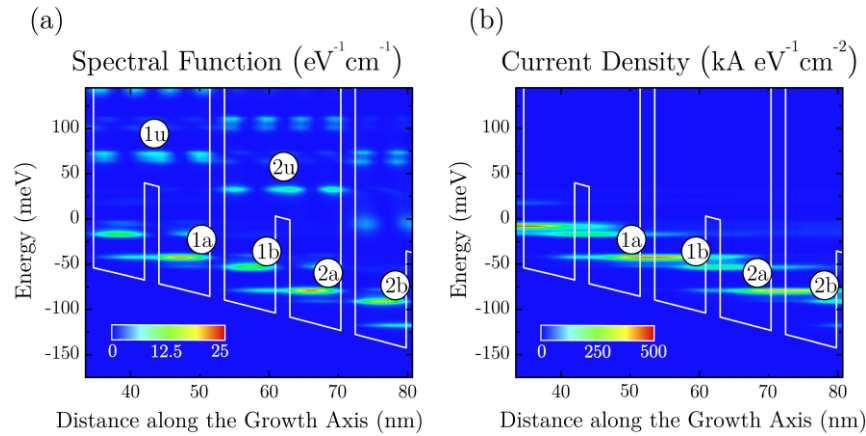


Fig. 1. Conduction band profile (white line) at the threshold voltage of 36 mV per period at  $T = 100$  K, and contour plots of the (a) energy and position resolved spectral function at vanishing in-plane momentum, and (b) energy and position resolved current density.

- [1] M. Büttiker, "Symmetry of electrical conduction", IBM J. Res. Develop. **32**, 317 (1988).
- [2] P. Greck, "Efficient calculation of dissipative quantum transport properties in semiconductor nanostructures", Selected Topics of Semiconductor Physics and Technology (G. Abstreiter, M.-C. Amann, M. Stutzmann, and P. Vogl, eds.), vol. 105, Verein zur Förderung des Walter Schottky Instituts der Technischen Universität München e.V., München (2012).
- [3] T. Kubis, C. Yeh, P. Vogl, A. Benz, G. Fasching and C. Deutsch, "Theory of nonequilibrium quantum transport and energy dissipation in terahertz quantum cascade lasers", Phys. Rev. B **79**, 195323 (2009).
- [4] T. Kotani (private communication) (2012).